

# Crystal Structures of Oligodeoxyribonucleotides Containing 6'- $\alpha$ -Methyl and 6'- $\alpha$ -Hydroxy Carbocyclic Thymidines<sup>†</sup>

Stefan Portmann,<sup>‡,§</sup> Karl-Heinz Altmann,<sup>||</sup> Nathalie Reynes,<sup>||,⊥</sup> and Martin Egli<sup>\*,:‡</sup>

Contribution from the Department of Molecular Pharmacology and Biological Chemistry, Northwestern University Medical School, Chicago, Illinois 60611-3008, Organic Chemistry Laboratory, ETH Swiss Federal Institute of Technology, CH-8092 Zürich, Switzerland, and Central Research Laboratories, CIBA Ltd., CH-4002 Basel, Switzerland

Received July 12, 1996<sup>⊗</sup>

**Abstract:** The X-ray crystal structures of two self-complementary DNA duplexes with the sequence d(CGCGAA<sub>t<sub>Me</sub>/OH</sub>t<sub>Me</sub>/OHCGCG) containing four 6'- $\alpha$ -methyl (t<sub>Me</sub>) or four 6'- $\alpha$ -hydroxy carbocyclic thymidines (t<sub>OH</sub>), respectively, have been determined. Both structures are isomorphous to the native Dickerson–Drew dodecamer duplex [d(CGCGAATTCGCG)]<sub>2</sub>. The cyclopentane moieties of the modified carbocyclic thymidine residues lacking the deoxyribose 4'-oxygen adopt either C2'-endo or C1'-exo B-DNA type puckers. The dodecamer duplex incorporating 6'- $\alpha$ -methyl carbocyclic thymidines shows an enlarged minor groove relative to both the unmodified duplex and the one with incorporated 6'- $\alpha$ -hydroxy carbocyclic thymidines. The pairing of oligonucleotides containing single or multiple 6'- $\alpha$ -substituted carbocyclic thymidines with complementary DNA is discussed on the basis of the structural data.

## Introduction

Inhibition of protein synthesis by the sequence-specific binding of an oligonucleotide to single-stranded (ss) RNA or double-stranded (ds) DNA targets ("antisense" and "antigene" approach, respectively) in the recent past has developed into an important novel approach in modern drug design.<sup>1</sup> Due to the insufficient metabolic stability of natural DNA and RNA under physiological conditions, the successful implementation of such oligonucleotide-based drug design strategies depends on the availability of chemically modified oligonucleotides or oligonucleotide analogs. These must not only exhibit largely increased resistance to nucleolytic degradation but also retain the ability to bind to their complementary target nucleic acids with high affinity and in a highly sequence-specific manner.<sup>1</sup>

As a consequence, a large variety of structurally modified oligonucleotide analogs have become known over the last few years and the effects of such structural modifications on nuclease resistance and RNA- or DNA-binding affinity have been investigated in some detail.<sup>1,2</sup> However, in contrast to the wealth of RNA- or DNA-binding data that have emerged from those studies, far less information is available on the changes in duplex

structure that are associated with covalent modification of the sugar–phosphate backbone of one of the component strands.<sup>3–6</sup> Changes in the ssRNA- or DNA-binding affinity of modified oligonucleotides do not necessarily have to reflect, or at least not exclusively so, structural changes in the Watson–Crick duplex but could also be related to conformational changes in the single strand.<sup>7,8</sup> However, it is very likely that any changes in the duplex structure that do actually occur will also affect duplex stability. The structural characterization of modified DNA/DNA and DNA/RNA duplexes should, therefore, not only improve our basic understanding of the structural properties of nucleic acid duplexes in general but it might also lead to the design of novel modifications with more favorable properties for therapeutic applications.

In this context we have embarked on a comprehensive program directed at the crystallographic investigation of nucleic acid duplexes incorporating sugar- and backbone-modified component strands. As part of these continuing studies, we now report on the structural properties of two modified analogs of the Dickerson–Drew dodecamer d(CGCGAATTCGCG), where both thymidine residues have been replaced either by 6'- $\alpha$ -

\* Author to whom correspondence should be addressed: MP&BC Department, Northwestern University Medical School; Phone (312) 503-0845; Fax (312) 503-0796; E-mail m-egli@nwu.edu.

<sup>†</sup> Coordinates for both crystal structures have been deposited in the Nucleic Acid Data Base; entry codes NDBS79 (MEME) and NDBS80 (OHOH).

<sup>‡</sup> Northwestern University Medical School.

<sup>§</sup> ETH Swiss Federal Institute of Technology.

<sup>||</sup> CIBA, Ltd.

<sup>⊥</sup> Summer Student from April to July 1994.

<sup>⊗</sup> Abstract published in *Advance ACS Abstracts*, February 15, 1997.

(1) (a) Uhlmann, E.; Peyman, A. *Chem. Rev.* **1990**, *90*, 543–584. (b) Milligan, J. F.; Matteucci, M. D.; Martin, J. C. *J. Med. Chem.* **1993**, *36*, 1923–1937. (c) *Antisense Research and Applications*; Crooke, S. T., Lebleu, B., Eds.; CRC Press, Inc.: Boca Raton, FL, 1993. (d) Altmann, K.-H.; Dean, N. M.; Fabbro, D.; Freier, S. M.; Geiger, T.; Häner, R.; Hüskén, D.; Martin, P.; Monia, B. P.; Müller, M.; Natt, F.; Nicklin, P.; Phillips, J.; Pieleus, U.; Sasmor, H.; Moser, H. E. *Chimia* **1996**, *50*, 168–176.

(2) (a) Varma, R. S. *Synlett* **1993**, 621–637. (b) De Mesmaeker, A.; Häner, R.; Martin, P.; Moser, H. E. *Acc. Chem. Res.* **1995**, *28*, 366–374. (c) De Mesmaeker, A.; Altmann, K.-H.; Waldner, A.; Wendeborn, S. *Curr. Opin. Struct. Biol.* **1995**, 343–355.

(3) For NMR spectroscopic studies on duplexes incorporating formacetal- and amide-type backbone modifications, respectively, cf.: (a) Gao, X.; Jeffs, P. W. *J. Biomol. NMR* **1994**, *4*, 17–34 (formacetal). (b) Blommers, M. J. J.; Pieleus, U.; De Mesmaeker, A. *Nucleic Acids Res.* **1994**, *22*, 4187–4194 (amide).

(4) For structural studies on duplexes incorporating peptide nucleic acids (PNA) strands, cf.: (a) Brown, S. C.; Thomson, S. A.; Veal, J. M.; Davis, D. G. *Science* **1994**, *265*, 777–780. (b) Betts, L.; Josey, J. A.; Veal, J. M.; Jordan, S. R. *Science* **1995**, *270*, 1838–1841.

(5) For X-ray crystallographic studies of self-complementary DNA duplexes containing 2'-O-methyladenosine and 4'-thiothymidine, respectively, cf.: (a) Lubini, P.; Zürcher, W.; Egli, M. *Chem. & Biol.* **1994**, *1*, 39–45 (2'-O-methyl ribose modification). (b) Boggon, T. J.; Hancox, E. L.; McAuley-Hecht, K. E.; Connolly, B. A.; Hunter, W. N.; Brown, T.; Walker, R. T.; Leonard, G. A. *Nucleic Acids Res.* **1996**, *24*, 951–961 (4'-thio modification).

(6) Recent X-ray crystal structure determinations of chemically modified oligonucleotide analogs have been reviewed Egli, M. *Angew. Chem., Int. Ed. Engl.* **1996**, *35*, 1894–1909.

(7) Schmit, C.; Bévierre, M.-O.; De Mesmaeker, A.; Altmann, K.-H. *Bioorg. Med. Chem. Lett.* **1994**, *4*, 1969–1974.

(8) Altmann, K.-H.; Imwinkelried, R.; Kesselring, R.; Rihs, G. *Tetrahedron Lett.* **1994**, *35*, 7625–7628 and references cited therein.

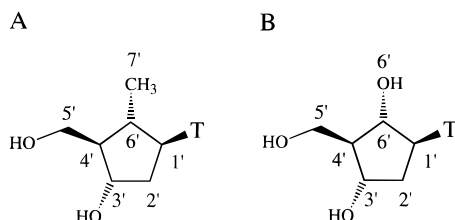


**Figure 1.** Structures and atom-numbering systems for 6'- $\alpha$ -substituted carbocyclic thymidine building blocks: MCT (A) and HCT (B).

methyl (MCT) or 6'- $\alpha$ -hydroxy (HCT) carbocyclic thymidines (Figure 1). Both of these modified building blocks have been previously investigated in the context of possible antisense applications. In these studies, oligonucleotides containing stretches of contiguous MCT residues were found to exhibit slightly reduced RNA-binding affinity (as compared to the unmodified wild-type parent sequences), while the incorporation of HCT led to increased DNA/RNA duplex stability.<sup>9,10</sup> However, in both cases the degree of nuclease resistance conferred to an adjacent phosphodiester bond does not suffice to produce significant biological effects with phosphodiester-based antisense oligonucleotides.<sup>9,10</sup> When the possible origins of the observed effects of MCT and HCT on RNA-binding affinity as well as the structural consequences associated with incorporation of these residues (at the single strand as well as at the duplex level) are contemplated, it should be remembered that the replacement of the furanose oxygen O4' by a carbon atom (designated C6', Figure 1) leads to the loss of the stereoelectronic effects influencing the conformation of the sugar moiety and renders the five-membered ring more flexible.<sup>11</sup> In addition, the solvation of oligonucleotides containing carbocyclic residues can be expected to be significantly different (at least at the site of the modification) from the unmodified parent duplex.

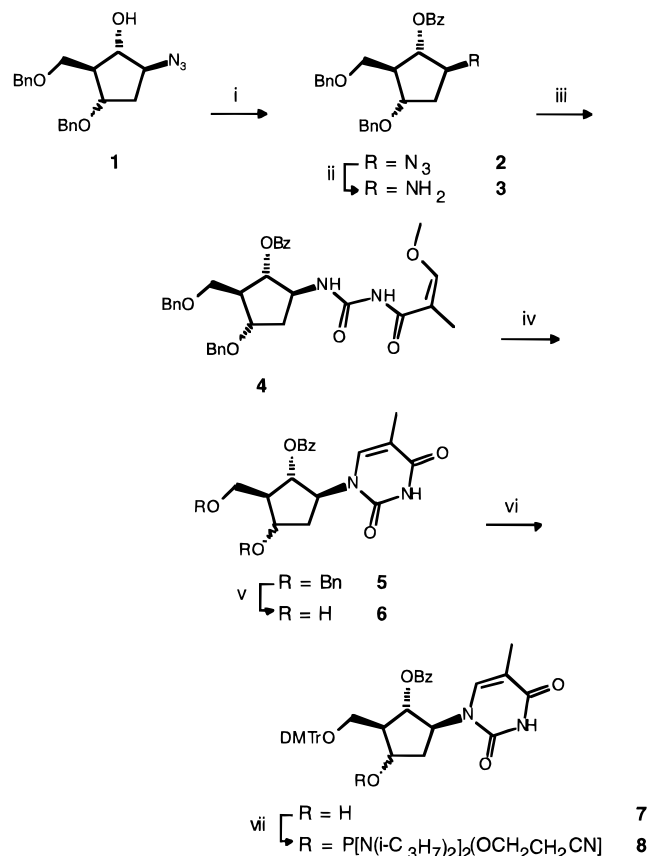
Here, we describe the crystal structures of the modified duplexes [d(CGCGAA<sub>t<sub>Me</sub>t<sub>Me</sub></sub>CGCG)]<sub>2</sub> (MEME; t<sub>Me</sub> = MCT) and [d(CGCGAA<sub>t<sub>OH</sub>t<sub>OH</sub></sub>CGCG)]<sub>2</sub> (OHOH; t<sub>OH</sub> = HCT) and compare them with the structure of the unmodified wild-type duplex. In addition, we describe the effects of MCT and HCT on DNA binding and try to analyze the DNA-binding affinity of HCT- and MCT-containing oligodeoxyribonucleotides in light of the structural properties of the two modified dodecamers.

## Materials and Methods

**Synthesis of Modified Nucleosides.** The synthesis of MCT together with that of the corresponding 5'-*O*-(4,4'-dimethoxytrityl) (DMTr) 3'-(2-cyanoethyl-*N,N*-diisopropylamino) phosphoramidite as required for oligonucleotide synthesis has been previously described.<sup>10</sup> The synthesis of HCT is based on the known azido alcohol **1** and is summarized in Scheme 1. Experimental details for the synthesis of 6'-OBz-HCT **5** and its derived 5'-*O*-(4,4'-dimethoxytrityl) (DMTr) 3'-(2-cyanoethyl-*N,N*-diisopropylamino) phosphoramidite **7** are contained in the Supporting Information.

**Oligonucleotide Synthesis.** Oligonucleotides were synthesized on an ABI 390b DNA synthesizer using long-chain alkylamino controlled pore glass (CPG, 500Å) and standard phosphoramidite chemistry (1.5  $\mu$ mol scale; 10  $\mu$ mol scale for modified Dickerson–Drew dodecamers).<sup>12</sup> Bases were protected by benzoyl (dC, dA) and isobutyryl (dG) groups. Extended coupling times of 10–12 min were employed for modified phosphoramidites, and no significant reduction in coupling

## Scheme 1<sup>a</sup>



<sup>a</sup> Key: i. BzCl, Et<sub>3</sub>N, CH<sub>2</sub>Cl<sub>2</sub>, rt, 18 h, 85%. ii. H<sub>2</sub>, Lindlar's catalyst, MeOH, rt, 6 h, 98%. iii. CH<sub>3</sub>OCH=C(CH<sub>3</sub>)CONCO, CH<sub>2</sub>Cl<sub>2</sub>, -60° → rt, 1.5 h, 97%. iv. 0.2 N HCl EtOH/H<sub>2</sub>O 9:1, reflux, 24 h, 74%. v. H<sub>2</sub>, 10% Pd-C, AcOEt/MeOH 1:1, rt 3 h, 87%. vi. DMTrCl, Et<sub>3</sub>N, DMAP (cat), pyridine, rt, 3 h, 67%. vii. [(i-C<sub>3</sub>H<sub>7</sub>)<sub>2</sub>N]<sub>2</sub>POCH<sub>2</sub>CH<sub>2</sub>CN, (i-C<sub>3</sub>H<sub>7</sub>)<sub>2</sub>NH<sup>+</sup>CHN<sub>4</sub>, CH<sub>2</sub>Cl<sub>2</sub>, rt, 2 h, 97%.

efficiency was observed under these conditions. After completion of chain assemblage, the 5'-*O*-DMTr-protected product was released from the support with concomitant cleavage of all protecting groups by treatment of the support-bound oligonucleotide with concentrated aqueous NH<sub>3</sub> for 16 h at 55 °C. The 5'-*O*-DMTr-protected products were purified by RP-HPLC, and the 5'-*O*-DMTr group was subsequently removed by treatment with 80% aqueous acetic acid for 30 min at room temperature (rt). For UV-melting studies, the deprotection mixture was evaporated to dryness and the residue was twice evaporated with EtOH/H<sub>2</sub>O 2:1. It was then redissolved in 2 mL of water and extracted twice with ether, and the solution was lyophilized. According to gel electrophoresis or capillary electrophoresis (CE), the fully deprotected oligonucleotides were at least 95% pure.

**Crystallization of Modified Oligonucleotides.** For crystallization experiments, four d(CGCGAATTCGCG)-type dodecamers with 6'- $\alpha$ -substituted carbocyclic residues were synthesized and subjected to crystallization trials. Rhombohedral crystals of the dodecamers d(CGCGA<sub>t<sub>OH</sub>t<sub>OH</sub></sub>CGCG) and d(CGCGA<sub>t<sub>OH</sub>t<sub>OH</sub></sub>CGCG) were disordered and diffracted only to low resolution. However, the orthorhombic crystals obtained with the MEME and OHOH dodecamers with two modified thymidines per single strand were isomorphous to the native DNA dodecamer and both diffracted X-rays to better than 2.5 Å resolution. They were grown from 1.0 mM DNA (1.2 mM for OHOH), 20 mM sodium cacodylate buffer pH 6.9, 18.8 mM Mg(OAc)<sub>2</sub>, and 0.7 mM spermine tetrahydrochloride, equilibrated against 40% 2-methyl-2,4-pentanediol (MPD), using the sitting drop vapor diffusion method. Data sets for both crystals were collected at room temperature with Cu K $\alpha$  radiation for the MEME dodecamer (crystal size 1.5  $\times$

(9) Altmann, K.-H.; Bévière, M.-O.; De Mesmaeker, A.; Moser, H. E. *Bioorg. Med. Chem. Lett.* **1995**, *5*, 431–436.

(10) Altmann, K.-H.; Kesselring, R.; Pielies, U. *Tetrahedron* **1996**, *52*, 12699–12722.

(11) For a comprehensive discussion of nucleic acid conformation, see: Saenger, W. *Principles of Nucleic Acid Structure*; Springer Verlag: New York, 1984.

(12) (a) Sinha, N. D.; Biernat, J.; McManus, J.; Köster, H. *Nucleic Acids Res.* **1984**, *12*, 4539–4557. (b) *Oligonucleotide synthesis - a practical approach*; Gait, M. J., Ed.; IRL Press: Oxford, 1984.

**Table 1:** Selected Crystal and Refinement Data

parameter	d(CGCGAAt <sub>Me</sub> t <sub>Me</sub> CGCG)	d(CGCGAAt <sub>OH</sub> t <sub>OH</sub> CGCG)
temperature	rt	rt
<i>a</i> (Å)	25.20	24.88
<i>b</i> (Å)	40.80	40.27
<i>c</i> (Å)	66.27	66.49
space group	<i>P</i> 2 <sub>1</sub> 2 <sub>1</sub> 2 <sub>1</sub>	<i>P</i> 2 <sub>1</sub> 2 <sub>1</sub> 2 <sub>1</sub>
resolution (Å)	2.50	2.14
<i>R</i> <sub>merge</sub> (%)	3.5	5.1
no. of reflections at a 2σ( <i>F</i> <sub>obs</sub> ) level used for refinement (10 Å to full resolution)	2072	3605
strands per asymmetric unit	2	2
vol./base pair (Å <sup>3</sup> )	1420	1388
no. of waters	65	66 + 1Mg <sup>2+</sup>
<i>R</i> -factor (%)	17.0	20.7
<i>R</i> <sub>free</sub> (%)	29.2	32.9
rms from ideality, bond lengths (Å)	0.018	0.017
rms from ideality, bond angles (deg)	3.70	3.36

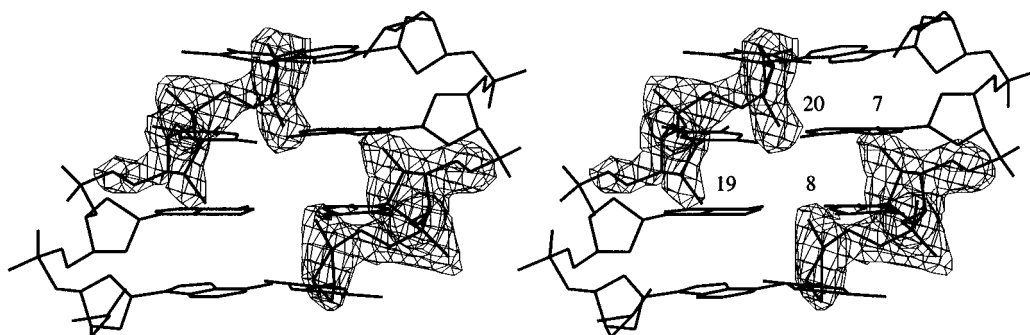


**Figure 2.** Stereodrawing of an omit electron density map contoured at 1.2σ around the sugar–phosphate backbone portions of residues OCT7, -8, -19, and -20 for OHOH (including all data to a resolution of 2.14 Å). The map was calculated with duplex coordinates minus the sugar portions of the four modified thymidines and the phosphates between them.

0.17 × 0.1 mm) on a Marresearch 300 mm image plate mounted on an Enraf-Nonius rotating anode generator and for the OHOH dodecamer (crystal size 0.5 × 0.2 × 0.2 mm) on an R-AXIS-II image plate mounted on a Rigaku rotating anode generator. Data were processed with the DENZO/SCALEPACK<sup>13</sup> program package and details concerning resolution and quality of the data sets are listed in Table 1.

**Structure Determinations and Refinements.** The unit cell constants and the space group of the MEME and OHOH crystals suggested isomorphism with the native DNA duplex [d(CGCGAATTCGCG)]<sub>2</sub><sup>14</sup> (NDB<sup>15</sup> Code BDL001). After initial rigid body refinement and several cycles of positional refinement with X-PLOR,<sup>16</sup> using the unmodified dodecamer duplex as a model for both structures, the additional exocyclic substituents appeared clearly in 2*F*<sub>obsd</sub> − *F*<sub>calcd</sub> sum and *F*<sub>obsd</sub> − *F*<sub>calcd</sub> difference electron density maps. The models were modified and the standard DNA restraints dictionary was adjusted. Following several cycles of refinement including a slow cooling procedure, water molecules were assigned to peaks appearing in both the sum and difference density maps. Water molecules that were accepted had to display good hydrogen-bonding geometry, be surrounded by 2*F*<sub>obsd</sub> − *F*<sub>calcd</sub> sum density at a 2σ level, and have a temperature factor of below 60 Å<sup>2</sup> after refinement. The latter two criteria were handled less strictly than the first. Refinement was terminated once no new water molecules could be added. In the OHOH structure a high-density region with octahedral shape in the sum and difference maps was interpreted as a

Mg<sup>2+</sup> ion with six coordinated water molecules. Refinement data are summarized in Table 1, and an omit density map around the modified residues in the OHOH duplex at the final stage is depicted in Figure 2.

**Two Crystal Forms.** Replacing Mg<sup>2+</sup> with Ca<sup>2+</sup> in crystallization solutions of both the MEME and OHOH dodecamers yields a new rhombohedral crystal form. Such crystals typically diffract X-rays to a resolution of 2.8 Å or less. Several other dodecamer strands with identical sequence, but containing either four 6′-unsubstituted or 6′-α-hydroxy carbocyclic residues at positions 6–9 or with the carbocyclic residues incorporated at locations other than T7 and T8, also crystallized in this rhombohedral form, even in the presence of Mg<sup>2+</sup>. However, crystals grown of the unmodified d(CGCGAATTCGCG) DNA dodecamer uniformly belong to the orthorhombic space group *P*2<sub>1</sub>2<sub>1</sub>2<sub>1</sub>, independent of whether the crystallization solutions are supplemented with Mg<sup>2+</sup> or Ca<sup>2+</sup>. In the lattice of the OHOH structure, a hydrated Mg<sup>2+</sup> ion is located between two adjacent symmetry-equivalent duplexes, whereby all six coordinated water molecules form direct contacts to DNA atoms. Three of them are hydrogen bonded to phosphate oxygens of a first duplex (O1P MCT7, O2P A6, and O1P A6), and the remaining ones form hydrogen bonds to major groove base atoms of a second duplex (N7 G2, O6 G2, and O6 G22).

**UV Melting Experiments.** With the exception of self-complementary sequences, melting temperatures (*T*<sub>m</sub> values) were determined in 10 mM phosphate buffer, pH 7, 100 mM Na<sup>+</sup>, 0.1 mM EDTA, at 4 μM strand concentration. The *T*<sub>m</sub> values for the modified Dickerson–Drew dodecamers as well as the wild-type oligonucleotide were recorded in 10 mM cacodylate buffer, pH 7, 100 mM NaCl, 0.1 mM EDTA, at 10 μM strand concentration, and the *T*<sub>m</sub> values are ±0.5°. For further experimental details, see ref 17.

(13) (a) Otwinowski, Z. Oscillation Data Reduction Program. In *Proceedings of the CCP4 Study Weekend: Data Collection and Processing*; Sawyer, L., Isaacs, N., Bailey, S., Eds.; SERC Daresbury Laboratory: England, January 1993; pp 56–62. (b) Minor, W. XDISPLAYF Program; Purdue University, 1993.

(14) (a) Wing, R.; Drew, H.; Takano, T.; Broka, C.; Tanaka, S.; Itakura, K.; Dickerson, R. E. *Nature* **1980**, *287*, 755–758. (b) Dickerson, R. E.; Drew, H. R. *J. Mol. Biol.* **1981**, *149*, 761–786.

(15) Berman, H. M.; Olson, W. K.; Beveridge, D. L.; Westbrook, J.; Gelbin, A.; Demeny, T.; Hsieh, S.-H.; Srinivasan, A. R.; Schneider, B. *Biophys. J.* **1992**, *63*, 751–759.

(16) Brünger, A. T.; Kuriyan, J.; Karplus, M. *Science* **1987**, *235*, 458–460.

(17) Lesnik, E. A.; Guinasso, C. J.; Kawasaki, A. M.; Sasmor, H.; Zounes, M.; Cummins, L. L.; Ecker, D. J.; Cook, P. D.; Freier, S. M. *Biochemistry* **1993**, *32*, 7832–7838.

(18) (a) Holbrook, S. R.; Dickerson, R. E.; Kim, S.-H. *Acta Crystallogr. B*, **1985**, *41*, 255–262 (NDB code BDLB05). (b) Westhof, E. *J. Biomol. Struct. Dyn.* **1987**, *5*, 581–600 (NDB code BDL020).

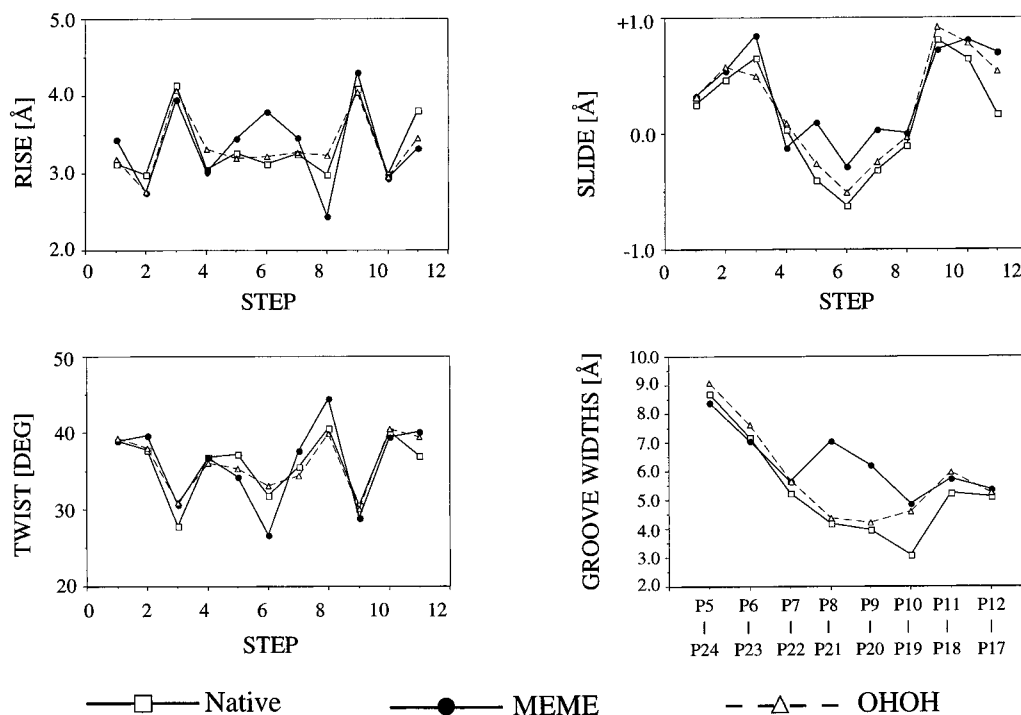


**Figure 3.** Helical rise, twist, slide, and minor groove widths of the  $[d(\text{CGCGAA}_{\text{tMe}}\text{tMeCGCG})_2]$  (MEME),  $[d(\text{CGCGAA}_{\text{tOH}}\text{tOHCGCG})_2]$  (OHOH), and  $[d(\text{CGCGAATTTCGCG})_2]$  (native, NDB code BDL001) duplexes. Helical parameters were calculated with the program NEWHEL93 distributed by R. E. Dickerson. The groove width is defined as the shortest distance between pairs of phosphorus atoms across the minor groove minus 5.8 Å, the sum of van der Waals radii for two phosphate groups.

## Results and Discussion

**Duplex Conformations.** Isomorphism of the two modified duplex crystals with those of the native B-DNA dodecamer duplex<sup>14</sup> is consistent with relatively small geometrical deviations between the three structures. The rms deviations between the Dickerson–Drew dodecamer and MEME and OHOH are 0.80 Å and 0.48 Å, respectively. The root mean square (rms) deviation between the MEME and OHOH structures is 0.64 Å. The smaller conformational difference between the OHOH and Dickerson–Drew duplexes, compared with the difference between the MEME duplex and the native one, are also apparent in a comparison of the helical and topological parameters of the three duplexes (Figure 3).

In accordance with the location of the modifications, the major geometrical differences between the duplexes occur in their central portions, particularly at the A6pT7 (A18pT19) step. There, the rise of MEME relative to the native duplex is increased by 0.68 to 3.80 Å and its twist is lowered by 5.1° to 26.7°. In addition, the base pairs are shifted in a positive direction (slide) in the three central base pair steps of the MEME duplex. Taken together, these changes result in an enlargement of the central minor groove by about 2.3 Å on average (Figure 3). The 7'-methyl substituents of the carbocyclic thymidines are directed into the central section of the minor groove and form the corners of an approximate square (Figure 4A). The distances between the C7'-carbon atoms within strands are 4.53 and 5.03 Å for strands 1 and 2, respectively, and they are 4.87 and 5.21 Å between carbon atoms from opposite strands. Thus, in terms of both their intra- and interstrand interactions, the methyl groups are in near van der Waals contact with one another. The minor groove widening is most likely caused by the bulky methyl groups.

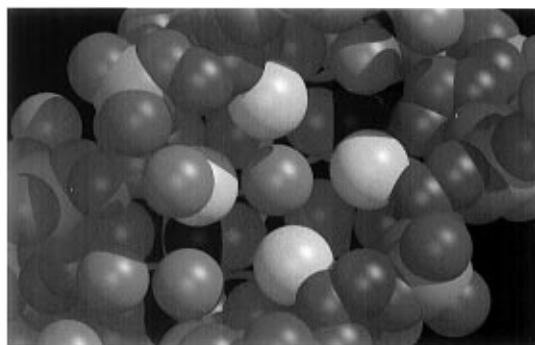
The helical parameters of the OHOH duplex are more similar to those of the native duplex, and their minor grooves display roughly the same widths (Figure 3). The only exception is constituted by the distance between the phosphorus atoms of

residues G10 and HCT19, which is slightly longer in OHOH than in the native duplex. In the minor groove of the OHOH duplex, the hydroxy substituents form the corners of a parallelogram (Figure 4B). The distances between the 6'-oxygens within strands are 4.65 and 4.80 Å for strands 1 and 2, respectively, and they are 4.70 and 4.82 Å between oxygen atoms from opposite strands. The shortest distance of 4.26 is observed along the short diagonal of the parallelogram between O6' of residue HCT8 and O6' of residue HCT20. Thus, the smaller and more polar 6'- $\alpha$ -substituents of HCT residues in the OHOH duplex are accommodated more smoothly within the B-DNA dodecamer structure and consequently do not alter the minor groove topology, while the more bulky methyl substituents of MCT residues in the MEME duplex distort the groove topology more severely.

**Conformations and Interactions of Carbocyclic Residues.** All 6'- $\alpha$ -substituted carbocyclic thymidines in the MEME and OHOH duplexes adopt either C2'-*endo*- or C1'-*exo*-puckers, resulting in pseudoequatorial positions of the 6'- $\alpha$ -substituents. The deoxyriboses of thymidines in the native structure have the lowest pseudorotation angle on average with many of them adopting C1'-*exo*-type pucker. The cyclopentane rings of carbocyclic thymidines in MEME display the highest pseudorotation angle values, indicative of C2'-*endo*-puckers, whereas those in OHOH lie between the *P* values of the native and the MEME duplexes (Figure 5). The two modified structures demonstrate that the cyclopentane ring of 6'- $\alpha$ -substituted carbocyclic residues can adjust smoothly to the geometrical constraints exerted by the furanosyl phosphate backbones and that they are fully compatible with B-form DNA.

The most drastic changes in the MEME backbone angles relative to those in the unmodified dodecamer duplex are observed in residues MCT7, MCT8, and C9 (Figure 5). The latter residue adopts a C3'-*endo*-pucker instead of the C1'-*exo* one in the native duplex. Its angle  $\alpha$  is changed from  $-sc$  to  $ap$ , angle  $\epsilon$  from  $ap$  to  $+sc$ , and angle  $\zeta$  from  $-sc$  to  $+sc$ . In

A



B



**Figure 4.** Views into the central portion of the minor grooves for the  $[d(CGCGAA_{M_{Mc}}CGCG)]_2$  (A) and  $[d(CGCGAA_{OH_{OH}}CGCG)]_2$  (B) duplexes. The included water molecules (cyan) have direct contacts to either DNA atoms (carbon green, oxygen red, nitrogen blue, phosphorus orange) or to first hydration-shell waters (distance criteria 3.4 Å). The exocyclic C7' methyl carbon and O6' hydroxyl oxygen atoms are highlighted in yellow and magenta, respectively. In both drawings, the strands comprising residues 19 (bottom) and 20 (top) are on the left, and the strands comprising residues 7 (top) and 8 (bottom) are on the right. Rotation of Figure 7 by 90°, such that the labels A–C are at the bottom, will generate an orientation of the duplexes that is identical to the one depicted here. Thus, the water molecule in the center of Figure 4A and the yellow carbon sphere to its immediate left represent the short C–H···O contact between W67 and the C7' methyl group of residue MCT19 in MEME (see Figure 7A). Similarly, the water molecule located between the two bottom magenta spheres in Figure 4B represents W67 bridging the 6'- $\alpha$ -hydroxyl groups of residues HCT19 and HCT8 across the minor groove of OHOH (see Figure 7B).

residue MCT8, angle  $\epsilon$  switches from *ap* to *-sc* and angle  $\zeta$  from *-sc* to *+sc*. In residue MCT7 angle  $\epsilon$  switches from *ap* to *-sc* and angle  $\zeta$  from *-sc* to *ap*. These alterations in the geometry of the sugar–phosphate backbone appear necessary to accommodate the 6'- $\alpha$ -methyl groups of the carbocyclic thymidines in the B-type duplex and together result in the opening of the minor groove.

As expected from the smaller changes in the overall structure of the OHOH duplex relative to the native one, their sugar–phosphate backbone geometries deviate only slightly, with the most notable change occurring at residue C9 adjacent to HCT8 (Figure 5). There, the  $\alpha$  and  $\gamma$  torsion angles are altered in a concerted way, the former angle from *-sc* to *+sc* and the latter from *+sc* to *-sc*. This crankshaft motion around torsion angle  $\beta$  may help to readjust the relative position of stacked base pairs at that site as a consequence of a subtle local conformational change induced by the 6'- $\alpha$ -OH modification. An interesting coincidence is the virtual lack of geometrical changes in the backbone of the second strands in the MEME and OHOH

**Table 2.** Geometry of the Hydrogen Bonds between HCT 6'- $\alpha$ -Hydroxyl Groups and N3 or O2 Atoms of Adjacent A or HCT Residues, Respectively, in the Minor Groove of the OHOH Duplex<sup>a</sup>

interaction <sup>b</sup>	HCT7– A6	HCT19– A18	HCT8– HCT7	HCT20– HCT19
<u>O6'</u> ···N3	2.89 Å	3.04 Å		
<u>C6'</u> – <u>O6'</u> –N3	112.2°	100.4°		
<u>O6'</u> – <u>N3</u> –C4	132.9°	141.3°		
<u>O6'</u> – <u>N3</u> –C4–N9	–26.8°	–24.6°		
<u>O6'</u> ···O2			2.64 Å	2.75 Å
<u>C6'</u> – <u>O6'</u> –O2			113.9°	106.8°
<u>O6'</u> – <u>O2</u> –C2			151.4°	147.9°
<u>O6'</u> – <u>O2</u> –C2–N1			–40.5°	–46.1°

<sup>a</sup> See also Figure 6. <sup>b</sup> Atoms of HCT residues are underlined.

structures. The only notable deviations from the native backbone geometry there are seen in residues MCT19 and HCT19, where the  $\epsilon$  angles are converted from *ap* to *-sc* and the  $\zeta$  angles from *-sc* to *ap*. This corresponds to a switch from the BI backbone conformational state to the BII one that had already been observed in the structure of a Dickerson–Drew dodecamer brominated at position C9 (NDB code BDLB04).<sup>19</sup> Packing forces in the orthorhombic crystal lattice are the most likely reason for the asymmetric geometrical changes in the backbone conformations of the MEME and OHOH structures. It is possible that such forces constrain the second strand to a larger extent, causing the duplex to adapt to the structural perturbations induced by the carbocyclic modifications mainly by altering its more flexible first strand.

In the OHOH structure, the 6'- $\alpha$ -hydroxyl groups of carbocyclic thymidines lie roughly in the planes defined by the bases of preceding residues and form hydrogen bonds to O2 and N3 atoms of T and A residues, respectively. In the first strand, the O6' of HCT7 is hydrogen bonded to N3 of A6 and the O6' of HCT8 is hydrogen bonded to the O2 of HCT7. Similarly, in the second strand, the O6' of HCT19 is hydrogen bonded to N3 of A18 and the O6' of HCT20 is hydrogen bonded to O2 of HCT19 (Figure 6). Hydrogen bonds between HCT and A residues display almost ideal geometries (Table 2). There, the N3 lone pairs of adenines are directed more or less at the 6'-hydroxyl groups of carbocyclic thymidines. The O6'–N3–C4 angles are 132.9° and 141.3° for the HCT7–A6 and HCT19–A18 interactions, respectively, and the small values for the improper torsion angles O6'–N3–C4–N9 indicate that the 6'- $\alpha$ -hydroxyl groups are practically positioned within the planes defined by the adenine bases (Table 2, Figure 6). By comparison, the hydrogen bonds between 6'- $\alpha$ -hydroxyl groups and exocyclic O2 atoms from thymidines are shorter, but the geometry at the acceptors is not ideal. The O6'–O2–C2 angles are 151.4° and 147.9° for the HCT8–HCT7 and HCT20–HCT19 interactions, respectively, and the larger values for the improper torsions O6'–O2–C2–N1 indicate that the 6'- $\alpha$ -hydroxyl groups are located further away from the planes defined by the thymine bases.

**Hydration.** In the central portion of the minor groove in the native B-DNA dodecamer duplex, a spine of hydration involving seven first hydration-shell water molecules was found to link guanine N3 or N2 and adenine N3 with cytosine and thymine O2 from opposite strands (Figure 7C).<sup>20</sup> Six second hydration-shell water molecules (not all shown in Figure 7C) then connect those with direct DNA contacts, leading to an uninterrupted network of water molecules. The 4'-oxygens

(19) Fratini, A. V.; Kopka, M. L.; Drew, H. R.; Dickerson, R. E. *J. Biol. Chem.* **1982**, *257*, 14686–14707 (NDB codes BDLB03 and BDLB04).

(20) Drew, H. R.; Dickerson, R. E. *J. Mol. Biol.* **1981**, *151*, 535–556.

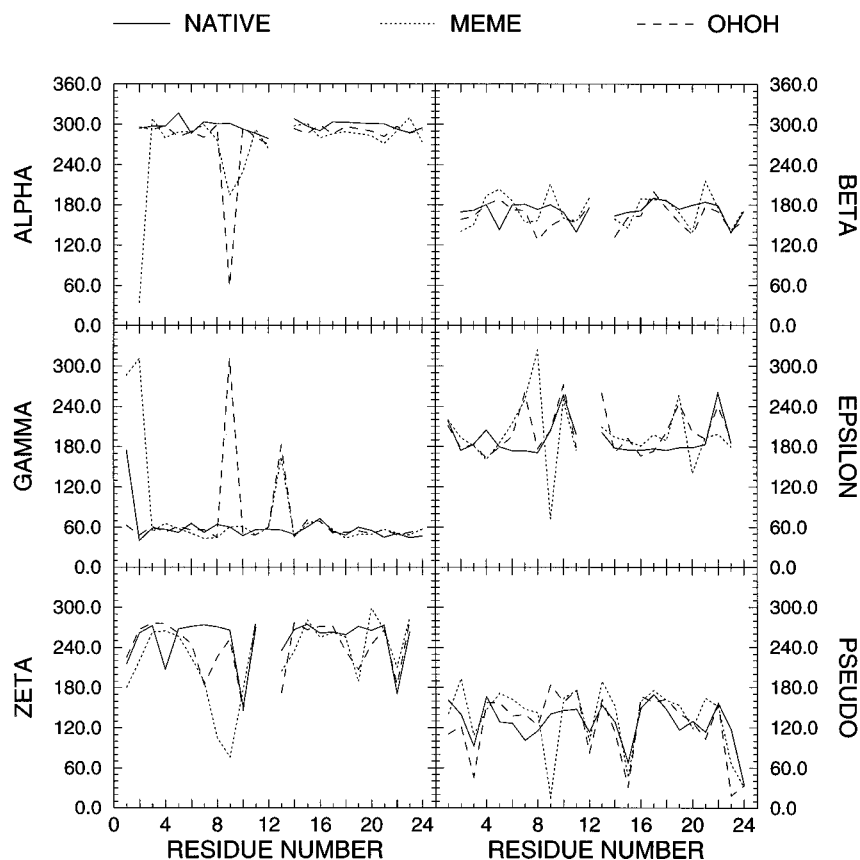


**Figure 5.** Backbone torsion angles and sugar pseudorotation phase angles  $P$  (in place of torsion angle  $\delta$ ) in  $[d(\text{CGCGAA}_{\text{Me}}\text{t}_{\text{Me}}\text{CGCG})]_2$  (MEME),  $[d(\text{CGCGAA}_{\text{OH}}\text{t}_{\text{OH}}\text{CGCG})]_2$  (OHOH), and  $[d(\text{CGCGAATTCGCG})]_2$  (native, NDB code BDL001). The statements in the text concerning the deviations in the sugar–phosphate geometry between this native unmodified duplex and the duplexes carrying the MCT and HCT modifications, respectively, are independent of the restraint parameters that were used for the refinements of the original structure<sup>15</sup> and subsequent ones.<sup>18,19</sup> Thus, the average backbone torsion angles (in degrees, omitting terminal base pairs) for the dodecamer structures with NDB codes BDL001, BDLB03, BDLB04, BDL005, and BDL020 are the following (standard deviations in parentheses):  $\alpha = 298.5(13.6)$ ,  $\beta = 170.4(15.1)$ ,  $\gamma = 52.7(12.8)$ ,  $\delta = 123.2(21.4)$ ,  $P = 130.4(28.9)$ ,  $\epsilon = 189.6(28.7)$ ,  $\zeta = 254.2(37.2)$ , and  $\chi = 244.1(15.3)$ . By comparison, the average angles and standard deviations when omitting BDL001 (our standard) are the following:  $\alpha = 298.6(14.8)$ ,  $\beta = 170.2(15.2)$ ,  $\gamma = 52.3(13.8)$ ,  $\delta = 123.2(22.2)$ ,  $P = 130.5(29.9)$ ,  $\epsilon = 189.7(29.6)$ ,  $\zeta = 254.2(38.0)$ , and  $\chi = 244.2(15.7)$ .

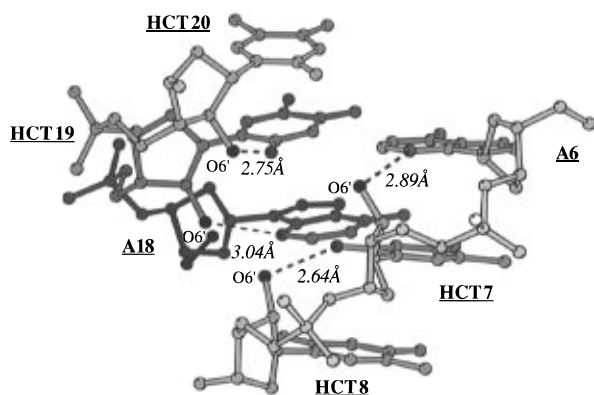


**Figure 6.** Hydrogen bonds between the 6'- $\alpha$ -hydroxyl groups (labeled) of carbocyclic thymidines and N3 or O2 atoms of 3'-adjacent A or HCT residues (bold and underlined), respectively, in the central portion of the minor groove of the  $[d(\text{CGCGAA}_{\text{OH}}\text{t}_{\text{OH}}\text{CGCG})]_2$  duplex. 6'- $\alpha$ -Hydroxyl oxygens are solid black, hydrogen bonds are dashed with their lengths given in italics, and darker portions of the duplex are further away from the reader.

contribute to a polar environment within the minor groove and are believed to stabilize the water spine.<sup>21</sup>

In MEME, the polarity near the floor of the minor groove is expected to change significantly as a result of the introduction

of 6'- $\alpha$ -methyl-substituted carbocyclic residues in the central portion of the duplex. If the furanose 4'-oxygens indeed contributed to the stabilization of the spine, their absence in portions of both strands in the MEME and OHOH duplexes should affect the geometry of the hydration spine. Comparison between the water positions in the native B-DNA duplex and MEME reveals that two second-shell water molecules are replaced by the four methyl groups in the latter structure (Figures 4A and 7A,C). In the terminology used by Drew and Dickerson,<sup>20</sup> these are water molecules w33 and w35, which bridge first-shell water molecules (throughout this section, water molecules in the native structure are in small font and water molecules in MEME or OHOH are in capital font). The first-shell water molecule W67 (w27 in the wild-type structure) is thereby isolated from the spine of hydration. This water is located in the center of the approximate square formed by the methyl groups, half-way between the periphery of the minor groove and its floor (Figure 4A). It forms hydrogen bonds to oxygens O2 of MCT7 and MCT19 and has a close contact of 3.12 Å to one of the 7'-methyl carbons (calculated  $[\text{C}]\text{H}\cdots\text{O}$  distance of 2.4 Å, Figure 7A). In the native structure, this water (w27) forms a weak hydrogen bond to the 4'-oxygen of T20 (3.38 Å) in addition to the above exocyclic keto oxygens; while in the modified structure, the corresponding W67 is slightly moved away from its native position, with an increased distance to the 6'-carbon of MCT20 (Figure 7A). Relative to the symmetrical arrangement of hydration spine water molecules

(21) Kopka, M. L.; Fratini, A. V.; Drew, H. R.; Dickerson R. E. *J. Mol. Biol.* **1983**, *163*, 129–146.



**Table 3.** Effect of 6'- $\alpha$ -Methyl Carbocyclic Thymidine (MCT) and 6'- $\alpha$ -Hydroxy Carbocyclic Thymidine (HCT) on the DNA Binding Affinities of Oligodeoxyribonucleotides ( $\Delta T_m$  values/modification<sup>a</sup>)

t	sequence <sup>b</sup>	$\Delta T_{m/mod}^a$	$T_m(WT)^c$
MCT	I	-1.7	43.0
HCT	I	-1.9	43.0
MCT	II	-1.6	62.5
HCT	II	-0.6	62.5
MCT	III	-1.1	58.2
HCT	III	-0.6	58.2
MCT	IV	-1.3	54.1
HCT	IV	-0.1	54.1
MCT	V <sup>d</sup>	-1.5	55.0
HCT	V <sup>d</sup>	-0.25	55.0

<sup>a</sup> Difference in melting temperature ( $\Delta T_m$ ) between the modified DNA/DNA duplex and the respective unmodified wild-type (WT) duplex divided by the number of modified building blocks ( $\Delta T_m = T_m - T_m(WT)$ );  $T_m$  values were determined in 10 mM phosphate buffer, pH 7, 100 mM NaCl, 0.1 mM EDTA, at 4  $\mu$ M strand concentration.

<sup>b</sup> Sequences are the following: **I** 5'-TTTTCTCTCTCTCT-3'; **II** 5'-tCCAGGtGtCCGCAtC-3'; **III** 5'-CTCGTACttttCCGGTCC-3'; **IV** 5'-GCGttttttttGCG-3'; **V** 5'-CGCGAAttGC $\overline{GC}$ -3'. <sup>c</sup> The  $T_m$  of the corresponding wild-type duplex in degrees Celcius. <sup>d</sup> Self-complementary sequence,  $T_m$  determined in 10 mM sodium cacodylate buffer, pH 7, 100 mM NaCl, 0.1 mM EDTA, at 10  $\mu$ M strand concentration.

hydration motif in our structure. Duplex destabilization appears to be slightly less pronounced for stretches of contiguous modified nucleotide units (Table 3, sequences III and IV;  $\Delta T_m = -1.1$  and  $-1.3$  °C per modification, respectively), which might be related to the release of water molecules in the vicinity of the methyl substituents combined with hydrophobic interactions between methyl groups in near van der Waals contacts. However, the subtleness of the effect makes it difficult to determine its precise structural origin.

With the exception of sequence I, DNA/DNA duplexes incorporating 6'- $\alpha$ -hydroxy-substituted nucleotide units in one of the component strands generally exhibit significantly higher thermodynamic stabilities (higher  $T_m$  values) than those containing the 6'- $\alpha$ -methyl carbocyclic modification. Hydrogen-bonding interactions between O6' atoms from HCT residues and O2 or N3 atoms from bases of adjacent residues as observed in the minor groove of the OHOH duplex could account for these differences. The 6'- $\alpha$ -hydroxyl groups of the HCT residues may thus be considered covalently bound water molecules, donating hydrogen bonds to base acceptor atoms in the minor groove. In addition, the difference in thermodynamic stability between the two self-complementary OHOH and MEME duplexes may also be attributed to the interstrand

bridging of 6'- $\alpha$ -hydroxyl groups in OHOH by water molecules (e.g., water W67, Figure 7B).

## Conclusions

The two crystal structures demonstrate that the cyclopentane moieties of 6'- $\alpha$ -substituted carbocyclic nucleotides can mimic the furanosyl conformation in a B-type DNA double helix and do not induce drastic changes in the overall duplex conformation. This is in agreement with the ability of modified DNA strands to form stable Watson-Crick base-paired duplexes with either complementary DNA or RNA strands. The modification that causes the smaller conformational deviations from the wild-type structure (i.e., 6'- $\alpha$ -hydroxy carbocyclic thymidine) generally leads to duplexes of higher stability. Perhaps surprisingly, the polar 6'- $\alpha$ -hydroxy substituent distorts the minor groove hydration more severely than the nonpolar 6'- $\alpha$ -methyl substituent. However, this adverse effect is compensated for by the 6'- $\alpha$ -hydroxyl groups constituting a covalent "first hydration-sphere" themselves and by their acting as hydrogen-bonding acceptors for additional water molecules at the groove periphery. It is noteworthy that the formation of these hydrogen bonds is sequence-independent, as all bases can in principle accept hydrogen bonds via either their N3 or O2 atoms from the 6'- $\alpha$ -hydroxyl groups. The presented work offers a structural rationale for the differences in thermodynamic stability between DNA/DNA duplexes incorporating either MCT or HCT modifications in one or both strands. Furthermore, OHOH and MEME add to the small database of crystal structures of oligonucleotides containing building blocks with chemically modified sugar moieties.<sup>5</sup>

**Acknowledgment.** We thank Dr. Fritz K. Winkler (Hoffmann LaRoche Ltd., Basel) for data collection with the MEME crystals, Dr. Uwe Piele and Werner Zürcher (CIBA Ltd., Basel) for oligonucleotide synthesis, and Dr. Dieter Hüsken (CIBA Ltd., Basel), Dr. S. M. Freier (ISIS Pharmaceuticals), and Dr. E. A. Lesnik (ISIS) for  $T_m$  measurements. We are also grateful to Dr. Sandro Hollenstein (University of Zürich) for help during the initial crystallization experiments, Dr. Valya Tereshko for producing Figure 2, and the two reviewers for helpful comments on the manuscript.

**Supporting Information Available:** Experimental and spectral details for 2-8 (4 pages). See any current masthead page for ordering and Internet access instructions.

JA962406A